RESEARCH ARTICLE

Determination of eddy dissipation rate by Doppler lidar in Reykjavik, Iceland

Shu Yang[1,2] | Guðrún Nína Petersen[2] | Sibylle von Löwis[2] |
Jana Preißler[3,4] | David C. Finger[1,5]

[1]School of Technology, Reykjavik University, Reykjavik, Iceland

[2]Icelandic Meteorological Office, Reykjavik, Iceland

[3]Centre for Climate and Air Pollution Studies, National University of Ireland, Galway, Ireland

[4]Leosphere, Saclay, France

[5]Sustainability Institute and Forum (SIF), Reykjavik University, Reykjavik, Iceland

Correspondence
Shu Yang, Reykjavik University, School of Technology, Reykjavik, Iceland.
Email: shu16@ru.is

Funding information
ISAVIA-the national airport and air navigation service provider of Iceland

Abstract

The temporal and spatial scale of atmospheric turbulence can be highly dynamic, requiring sophisticated methods for adequate detection and monitoring with high resolution. Doppler light detection and ranging (lidar) systems have been widely used to observe and monitor wind velocity and atmospheric turbulence profiles as Doppler lidar systems can provide continuous information about wind fields. The use of lidars in the subarctic region is particularly challenging as aerosol abundance can be very low, leading to weak backscatter signals. In the present study, we analysed data collected with a Leosphere Windcube 200S lidar system stationed in Reykjavik, Iceland, to estimate the eddy dissipation rate (EDR) as an indicator of turbulence intensity. For this purpose, we retrieved radial wind velocity observations from velocity–azimuth display scans and computed the EDR based on the Kolmogorov theory. We compared different noise filter thresholds, scan strategies and calculation approaches during typical Icelandic weather conditions to assess the accuracy and the uncertainty of our EDR estimations. The developed algorithm can process raw lidar observations, retrieve EDR and determine the qualitative distribution of the EDR. The processed lidar observations suggest that lidar observations can be of high importance for potential end-users, for example air traffic controllers and aviation safety experts. The work is an essential step towards enhanced aviation safety in Iceland where aerosol concentration is in general low and severe turbulence occurs regularly.

KEYWORDS
eddy dissipation rate, ground-based remote sensing, Iceland, lidar, observations, turbulence, wind

1 | INTRODUCTION

Extreme weather phenomena can have hazardous impacts on aviation safety. In particular, rapid changes in

headwinds and crosswinds during aircraft take-off or landing can lead to critical situations, which may jeopardize human lives. This is due to the low airspeed and low altitude of aircraft, only allowing minor corrective measures to be made to adjust for turbulence (Hon and Chan, 2014). According to the safety report of the International Civil Aviation Authorities (ICAO), more than one-third of aircraft accidents in 2017 occurred during take-off and landing (ICAO, 2018).

Iceland, located in the North Atlantic Ocean, is well known for extreme and highly variable weather conditions with frequent strong winds and gusts exceeding $25~m·s^{-1}$ (Ólafsson and Ágústsson, 2007; Ólafsson et al., 2007). This often raises aviation safety concerns. However, the frequency of high crosswinds has also made Keflavik International Airport an ideal location for aircraft manufacturers to test new aircraft (Norris, 2019). Thus, weather conditions in Iceland make the detection of turbulence for enhanced aviation safety a priority.

Any small scale, irregular air motion, that is, rapid irregular change in wind direction and/or speed, can be considered atmospheric turbulence. Atmospheric turbulence can be generated by mechanical processes such as wind shear, surface roughness, friction, wind jets, and obstacles or thermal processes such as buoyancy produced by surface heating or cloud-top radiative cooling. Accordingly, turbulences are directly related to surface roughness and atmospheric stability.

The scale of atmospheric eddies ranges from the synoptic scale (thousands of kilometres) to microscale (tens of metres). The eddies that affect aviation the most have a spatial scale between about 100 m and 1 km (Sharman, 2016). Conventional instruments such as anemometers mounted on meteorological masts can detect local turbulence only at the location of the instrument, providing limited information about the spatial distribution of turbulence in the vicinity of airports. On the other hand, radio soundings, which measure a vertical profile through the atmosphere, may reveal the vertical distribution of turbulence but are limited to when and where the sonde is released. To detect and quantify turbulence and obtain a clear picture of the wind conditions, several international airports, for example Hong Kong (Chan, 2010) and Sendai (Misaka et al., 2008), have added light detection and ranging (lidar) systems to their Aviation Weather Observation Systems.

The use of commercial lidars for ground-based remote sensing of wind has become increasingly important in the last decade (Sathe and Mann, 2013). In addition to being used in the aviation sector (Hon and Chan, 2014; Leung et al., 2018), lidars are also widely used in the wind energy sector (Wächter and Rettenmeier, 2009) as well as in wind-related meteorological research (Tuononen et al., 2017; Manninen et al., 2018). Compared

to the use of in situ methods like anemometers and radio sounding, lidars have the advantage of making continuous measurements with high temporal and spatial resolution. Lidars also allow the monitoring of wind fields within and above the boundary layer without the need for masts. Furthermore, tall masts may not be desirable in some places, for example at airports. Another advantage is that lidars are quite compact and mobile and therefore can be deployed at different locations.

Previous studies focusing on turbulence detection using Doppler lidars have encompassed investigations ranging from a purely theoretical approach to practical research. Frehlich (2001), Frehlich and Cornman (2002) and Frehlich et al. (2006) reported their development of a method to estimate turbulence intensity from the Kolmogorov theory, while Smalikho and his colleagues explored turbulence detection by continuous wave and pulsed Doppler lidars (Smalikho et al., 2005; Smalikho and Banakh, 2017; Stephan et al., 2018). In Europe, several studies have been conducted on the retrieval of eddy dissipation rate (EDR) as the indicator of turbulence intensity from lidar datasets, although some use ε ($m^2·s^{-3}$), for example O'Connor et al. (2010), and some use $\varepsilon^{-1/3}$ ($m^{2/3}·s^{-1}$), for example Thobois et al. (2015) and Muñoz-Esparza et al. (2018). At Hong Kong International Airport, lidars have been applied to detect low-level turbulence (Chan, 2009; Hon and Chan, 2014; Leung et al., 2018). However, the use of lidars for turbulence intensity detection in high latitude regions, such as in Iceland, has received little attention. The atmospheric turbulence in Iceland is typically characterized by strong wind fields, weather fronts, accentuated wind shear and blizzards. The volcanic geology leads to additional turbulence near the numerous steep mountains and low temperatures result in a shallow mixing layer. All these factors make the application of lidar observations in Iceland relevant and urgent. However, the atmosphere is often relatively clean, which may reduce the backscatter signal of emitted light pulses and result in a reduction of the range of the lidar measurement.

O'Connor et al. (2010) developed an algorithm to retrieve EDR from vertical lidar scans, hereafter called vertical stares, as the beam is kept in the vertical position. However, the horizontal wind velocity is generally an order of magnitude larger than vertical velocity and of importance for aviation due to the headwind and tailwind variations (Sinclair and Kuhn, 1991) as well as high crosswinds. Accordingly, in the present study we develop an algorithm to retrieve the EDR as an indicator of turbulence intensity from horizontal wind measurement by lidar in Reykjavik, Iceland.

We used a Leosphere Windcube 200S Doppler lidar system (Leosphere, 2013) located at the headquarters of the Icelandic Meteorological Office (IMO) in Reykjavik,

Iceland. The results are compared to vertical stares using the method of O'Connor *et al.* (2010). Additionally, we discuss different data filtering methods and compare two calculation approaches.

2 | METHODOLOGY

2.1 | Instruments

Two identical lidar systems, Leosphere Windcube 200S Doppler scanning lidars with depolarization functionality, are currently in operation in Iceland (Table 1). One system is located at Keflavik International Airport and the other system is a mobile system, installed on a trailer. In the present study, we only used data from the mobile system, which was located at IMO's headquarters in Reykjavik (64.1275 ° N, 21.9027 ° W) for the duration of this study. The site is an urban location in the centre of the capital region and the local impact on the wind climate is due to buildings and urban vegetation.

A Doppler lidar can measure radial wind speed along the beam based on the Doppler effect, often termed Doppler velocity. Using the Doppler lidar system we can retrieve profiles of wind speed and wind direction and estimate the EDR, as explained in detail in Section 2.3.

2.2 | Scan settings

The lidar systems can be programmed to scan the surrounding atmosphere. The scan strategy used in the present study was as follows:

TABLE 1 The specifications of the lidars operated in Iceland (Leosphere, 2013)

	Specification
Company	Leosphere – a Vaisala company
Website	http://www.leosphere.com
Model	Windcube 200S
Wavelength	1.54 μm
Maximum power	5 mW
Pulse width	200 ns
Range resolution	50 m
Pulse rate frequency	20 kHz
Maximum detection range	12 km
Minimum detection range	100 m
Azimuthal angle range	0–360°
Elevation angle range	−10°–190°

- Every 15 min two 360° revolution conic shaped velocity–azimuth display (VAD) scans were performed at elevation angles of 75° and 15°.
- The transverse interval (azimuthal resolution) during the VAD scans was 30°, resulting in 12 beams for each scan. The accumulation time for each beam was 5 s. In total, one conic VAD scan with 12 beams took approximately 70 s (including 10 s due to the change in azimuth angles).
- Between VAD scans, vertical stares were performed continually with a 1 s accumulation time per profile.

As the lidar measures the radial wind velocity, along the line of sight, both vertical stares and VAD scans can acquire information on the EDR. First, we focus on the VAD scans and an approach that has been documented extensively in the literature (see for example Frehlich *et al.*, 2006; Hon and Chan, 2014; Thobois *et al.*, 2015). The horizontal wind component, which is of importance for aviation safety and the focus of this study, can be derived from the VAD scans, while the data from vertical stares is only used as a verification reference in the present study.

2.3 | Theory on turbulence estimation

Turbulence is defined as a highly irregular movement of fluid. Given the range of length and time scales of eddies, it is challenging to describe the motion physically. One approach to measure turbulence is using the Kolmogorov theory (Kolmogorov, 1962; 1991). According to the Kolmogorov theory, energy is injected into the turbulent medium from the larger spatial scales and forms eddies. Eddies break down into smaller eddies until the kinetic energy is dissipated to thermal energy by the viscous properties of the medium. The dissipation rate, that is, the EDR, can therefore be used as a turbulence intensity indicator (Hocking, 1985; Cohn, 1994). There are several approaches to retrieve the EDR value from lidar observations. For example, Frehlich and Cornman (2002) estimated the EDR and the length scale from velocity data while Nijhuis *et al.* (2019) compared different methods to retrieve the EDR from wind velocity, obtained from Doppler radar. Also, Smalikho and Banakh (2017) estimated the EDR using the azimuthal structure function and Thobois *et al.* (2015) explored the possibility of estimating EDR by using a Leosphere Windcube lidar in Toulouse, France. In the present study, we developed an algorithm to estimate the EDR by using the velocity structure function and applied the algorithm to our lidar data obtained in Reykjavik. This method is based on the Kolmogorov theory (Frehlich, 2001), which assumes that

the atmosphere is isotropic and homogeneous over the observation domain. In Section 3.1 we discuss the homogeneity of the atmosphere.

The radial velocity V_r, as measured by a Doppler lidar, can be given by:

$$V_r = U \sin\varphi \cos\theta + V \cos\varphi \cos\theta + W \sin\theta \qquad (1)$$

where U, V and W are the wind components in m·s^{-1} in the x, y and z directions, φ is the azimuthal angle (with $0°$ pointing to the north) and θ is the elevation angle (with $90°$ pointing vertically) (Figure 1). With a fixed elevation angle scan, the radial velocity V_r is a sinusoidal function of the azimuthal angle. Finding the fitting parameters of the observed values with respect to this model gives us the 3D wind field. The coefficient of determination R^2 can be used as an indicator of the homogeneity of the atmosphere (Päschke et al., 2015), defined as:

$$R^2 = 1 - \sum_i \left(V_{ri} - \tilde{V}_{ri}\right)^2 / \sum_i \left(V_{ri} - \bar{V}_r\right)^2 \qquad (2)$$

with $\tilde{V}_{ri}$ denoting the radial velocities from the sine fit, or theoretical velocities, and $\bar{V}_r$ denoting the average of the measured radial velocities V_{ri} of one VAD scan ($i = 1, 2, ..., 12$). Larger R^2 values indicate that the VAD velocity is close to the sine fit, which means that the atmosphere is approximately homogeneous.

If the atmosphere is homogeneous and isotropic, the Kolmogorov theory can be applied and the energy spectrum (power density as a function of frequency) should fit a $-5/3$ slope (Figure 2):
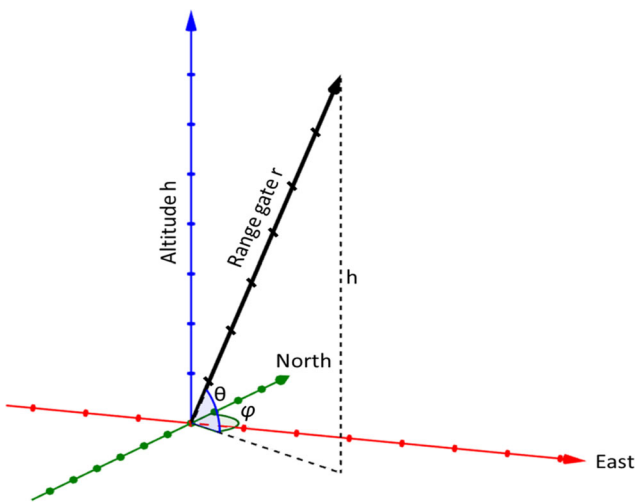
$$E(k) = C\varepsilon^{2/3} k^{-5/3} \qquad (3)$$

where C is the Kolmogorov constant, ε is the EDR and k is the wavenumber, which is proportional to frequency f.

If the atmosphere is isotropic and the slope of the power density to the frequency in a log–log figure is close to $-5/3$ (Figure 2), a direct relationship between the energy spectrum $E(K)$ and the structure function D_v can be defined (Frehlich et al., 2006; Thobois et al., 2015). For a scanning lidar, the EDR (ε, in m^2·s^{-3}) can be obtained by fitting the $-5/3$ slope to the structure function, leading to:

$$D_v = C_v \varepsilon^{2/3} s^{2/3} \qquad (4)$$

where $C_v \sim 2$ is the Kolmogorov constant.

The velocity structure function D_v is given by:

$$D_v = \left\langle \left[v'(r) - v'(r+s)\right]^2 \right\rangle \qquad (5)$$

where

$$v'(r) = v(r) - \langle v(r) \rangle \qquad (6)$$

are the fluctuations from the mean velocity $\langle v(r) \rangle$ at a specific range gate r, which should follow the fitted sine curve (Frehlich et al., 2006), and s is the spatial difference. The curve fit varies for different range gates; it is

FIGURE 1 A schematic of the lidar beam vector (black). The azimuth angle φ is shown in green with north being $0°$ and the elevation angle θ in blue with $90°$ representing a vertical beam. H is the altitude of the range gate and r is the distance along the beam
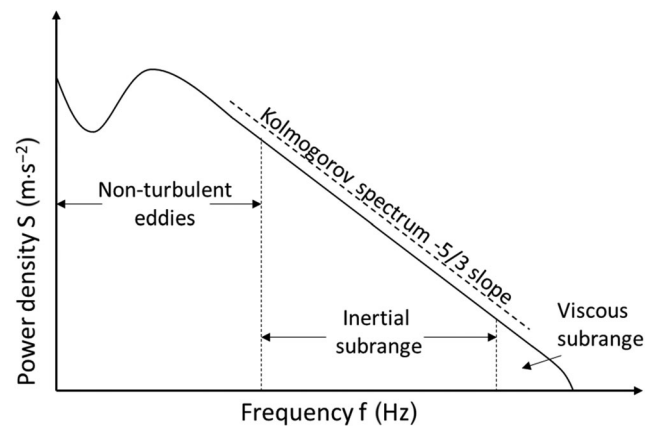

FIGURE 2 A schematic of the wind velocity power density as a function of frequency conforming to Kolmogorov's hypothesis. The inertial subrange is the part of the power spectrum where energy is transferred to smaller scales by turbulence. For 3D turbulence, the power spectrum is theoretically proportional to $k^{-5/3}$, where k is the wavenumber. Redrawn from O'Connor et al. (2010) and Thobois et al. (2015)

typically better at lower range gates where there is less noise. The distance to range gate r can easily be converted to height h using trigonometric functions.

The structure function can be estimated either along a transverse direction (one azimuth angle to another), which is the azimuthal approach, or along the lidar beam direction (one range gate to another), which is the longitudinal approach. Accordingly, s varies based on the approach: for the azimuthal approach it is the distance between the two points at the same range gate on adjacent beams ($s = r \sin(\Delta\varphi) \sin[0.5(\pi - \Delta\varphi)]^{-1}$, $\Delta\varphi$ is the azimuthal interval), which varies between range gates, and for the longitudinal approach it is equivalent to the range gate width, which is 50 m in the present study. Thus, to calculate the average value using the azimuthal approach, 12 profiles are averaged at each range gate. In contrast, for the longitudinal approach, a moving average is applied along each profile. A comparison between the two approaches is presented in Section 4.

Besides the VAD scans, data from the vertical stares were used in the present study for verification, applying the method of O'Connor *et al.* (2010). This work retrieved EDR based on the same theory but used the Doppler velocity variances of vertical stares combined with estimated horizontal wind speed, which gives an estimation of length scale.

3 | DATA EXPLOITATION

3.1 | Data screening

The radial wind velocity dataset from the lidar contains scan information, time, measured radial velocity, deviation of radial velocity, carrier-to-noise ratio (CNR) and confidence index (CI). We selected 2 days for case studies: March 24, 2017, as the turbulent case and March 31, 2017, as the calm case.

First, we investigated if the observed velocity energy spectra, derived from vertical stare data using a fast Fourier transform method, agreed with the expected $-5/3$ slope. The shape of the measured energy spectrum depends not only on the meteorological conditions and altitude but also on the airflow directions (Pauscher *et al.*, 2016). In general, the energy spectrum fits the idealized slope better at a lower altitude, due to the distribution of energy pulses over ranges. Figure 3 shows two examples of 1 hr vertical stare data on March 24, 2017, at different altitudes (450 and 1950 m). As expected, the lidar performs poorly on wind velocity with a weaker signal at higher heights (Frehlich, 2001). The lidar signal is governed by the signal backscattering from particles in the atmosphere. Thus, signal quality is better at a lower altitude, where the aerosol concentration is high (Ramanathan *et al.*, 2001). In high latitude regions like
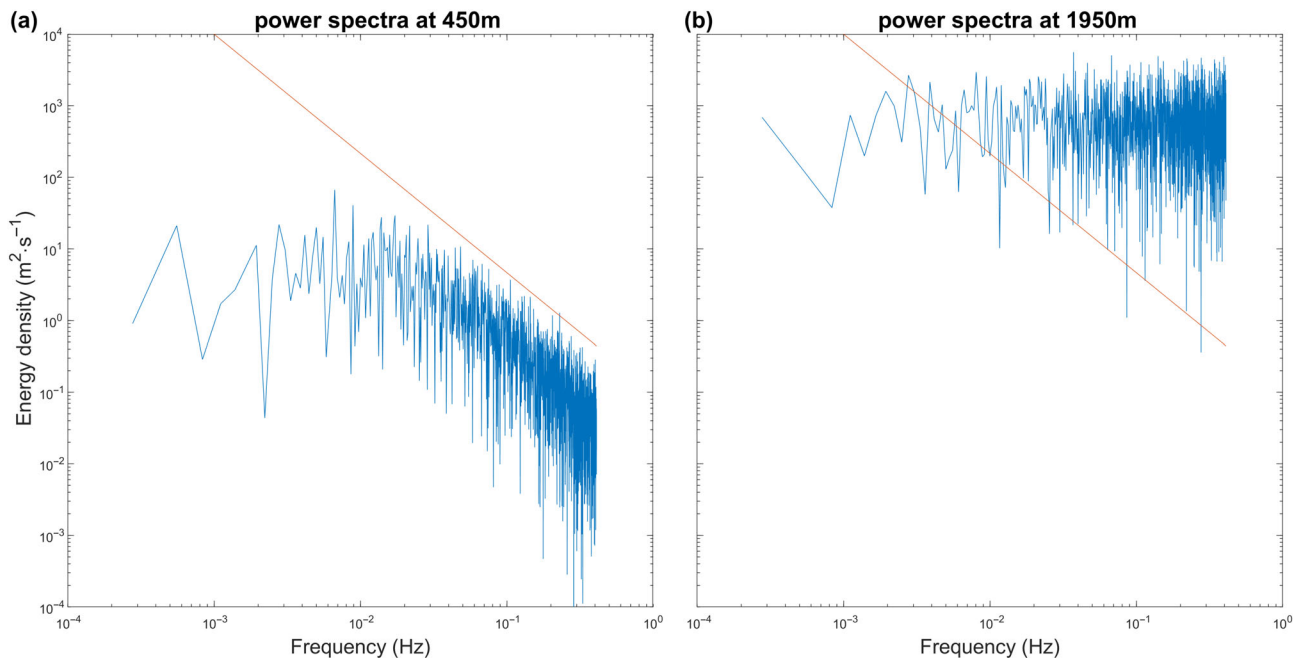

FIGURE 3 Verification of data quality: the velocity energy spectrum (blue curve, derived from the vertical velocity profile) should correspond to a $-5/3$ slope (red line). A good example (a) versus a bad example (b) from the same day (March 24, 2017). Data from different altitudes (450 m for (a) and 1950 m for (b)). Both are averaged over 1 hr (1600 to 1700). The mean carrier-to-noise ratio value is -4.3 dB (a) and -32 dB(b)

Iceland, the mixing layer is generally shallower than at continental mid-latitude sites, and the number of scatterers is relatively small (O'Connor, 2017). This explains the lower CNR at a high range and it may also contribute to the bias.

In general, we use CNR as an indicator of the backscatter signal intensity. The CNR depends on the backscatter and extinction coefficient of atmospheric aerosols (Boquet *et al.*, 2016), and a high CNR is expected with increasing aerosol load. Weather conditions, for example the mixing process, also impact the CNR level. In the cases shown in Figure 3, the mean CNR is −4.3 dB at 450 m and −32 dB at 1,950 m height above ground. To exclude the impact of noise, the CNR is used for data screening in many studies (Boquet *et al.*, 2016; Gryning *et al.*, 2016; 2017). In addition to using the CNR to screen noise and invalid data, the CI can also be applied. Radial wind at each time and range step is determined by computing the spectrum using a fast Fourier transform method, and subsequently fitting this spectrum to a theoretical curve. The CI threshold depends on the CNR, mean error and spectrum broadening of this spectral fit. The CI is factory calibrated individually for each lidar system and each range gate length. The calibration requires a few hours of noise measurements, where outgoing radiation is shielded from the receiver telescope. The CI threshold is then set to a value that limits the false positive rate to 0.25% (Dabas, 1999). For the scans applied here, the CI is a binary quality control parameter returning the value 0 for rejected data points and 100 for valid data points.

Manninen *et al.* (2016) estimated the uncertainty introduced by noise when they quantified turbulence intensity from lidar data and they developed a background correction algorithm to increase data availability. We applied this algorithm on the lidar data from vertical stares, but it is not implemented for VAD scans. The most commonly used CNR threshold for other lidar systems is −22 dB (Frehlich, 1996; Gryning *et al.*, 2016; 2017) or −27 dB for Windcube 200S (Boquet *et al.*, 2016). However, there are indications that those thresholds might be too high for Iceland since the atmosphere is often quite clean and, subsequently, the number of scatterers small. To determine the best data screening threshold for our lidars, we implemented a sensitivity test of different CNR values and CI values. We applied different thresholds to data obtained on two selected dates, and then calculated the data availability (DA = (available datapoints/ totaldata points) × 100%) and mean R^2 value (see Equation 2). A larger DA value indicates more data points were kept, while a larger R^2 value indicates that the kept data points have a higher quality (based on the fit to the sine curve, see Section 2.3). In general, a higher CNR

threshold results in improved data quality (larger R^2 value) but fewer data points (smaller DA value). This is to be expected as there is always a trade-off between data availability and data quality when determining an optimal CNR threshold. Figure 4 shows results from a sensitivity test of data quality and availability, depending on the CNR. We found that during a turbulent day the data quality and amount of data retrieved are higher than during a calm day, and low elevation scans have improved data quality compared to high elevation scans. This is reasonable since the atmosphere is better mixed on turbulent days and more scatterers are expected at lower altitudes since the main source of scatterers is the surface. In our study, we used a CNR threshold of −32 dB because this corresponds to a cut-off point for DA and the R^2 value changes for every curve in Figure 4: the improvement of R^2, and the decrease of DA, is less
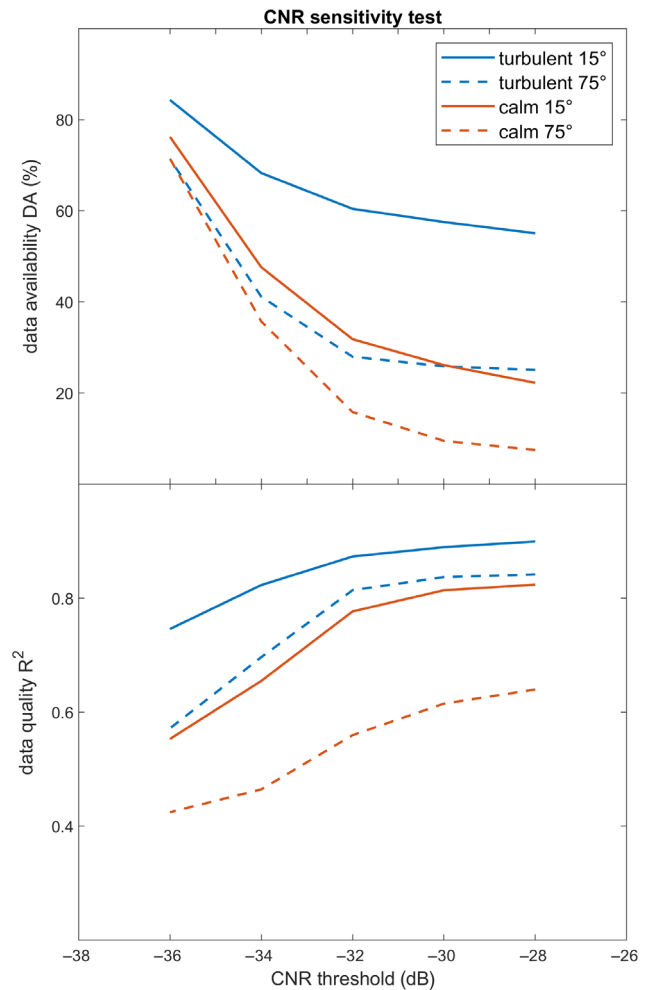

FIGURE 4 Carrier-to-noise ratio (CNR) sensitivity test results. Blue and red curves represent the data availability on a turbulent and calm day, March 24 and March 31, 2017, respectively. The solid lines indicate velocity–azimuth display scans at a 15° elevation angle and the dashed lines at a 75° elevation angle

TABLE 2 Comparison of data availability (DA) and R^2 for carrier-to-noise ratio (CNR) and confidence index (CI) thresholds applied on data from a turbulent day (March 24, 2017) and a calm day (March 31, 2017) at two elevation angles

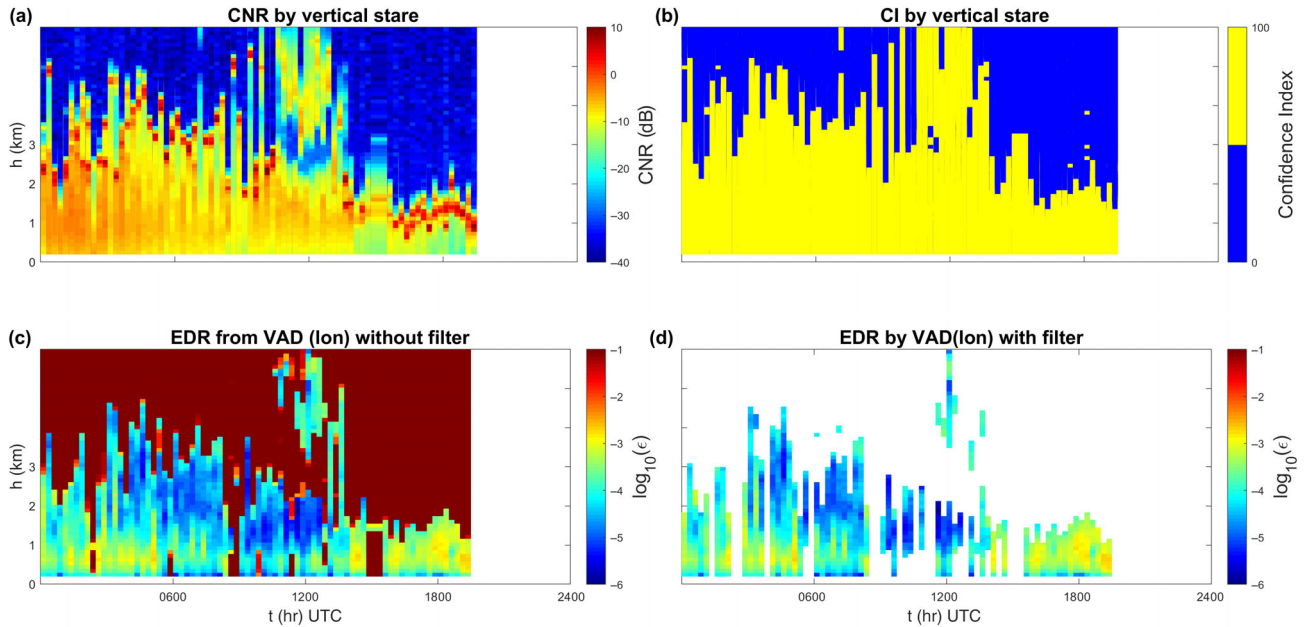| Date	March 24, 2017				March 31, 2017			
Elevation angle	15°		75°		15°		75°	
CNR	DA (%)	R^2	DA (%)	R^2	DA (%)	R^2	DA (%)	R^2
−30	57.54	0.8895	25.85	0.8370	26.13	0.8139	9.51	0.6150
−32	60.43	0.8731	27.97	0.8140	31.82	0.7768	15.82	0.5597
CI = 100	58.91	0.8826	26.55	0.8303	28.73	0.8020	12.04	0.5952

FIGURE 5 Carrier-to-noise ratio (CNR) in dB (a), the confidence index (CI) (b), the base-10 logarithm of eddy dissipation rate (EDR, $m^2 \cdot s^{-3}$) without filter (c) and with filter (d) on March 24, 2017. The EDR is derived from the velocity–azimuth display (VAD) scans, at a 75° elevation angle and using the longitudinal approach. Note that, in this case, no data are available after 2000 UTC

sensitive when the CNR is larger than −32 dB, compared to smaller than −32 dB.

As the CI is provided by the lidar system and it depends on the factory settings, we cannot investigate its sensitivity. In Table 2 we present a comparison between the CNR and CI thresholds. The CI threshold corresponds to a CNR threshold between −32 and −30 dB. In the present study we used a combination of CNR ≥ −32 dB and CI = 100. Any data points which do not meet these conditions were discarded.

Figure 5 displays the effect of the data screening filter. Figure 5a,b shows the CNR and CI on March 24, 2017. The calculated EDR (longitudinal approach) without any filter is shown in Figure 5c, and the result of data screening applied before calculating EDR is shown in Figure 5d. The figure shows that, while the filter removes noise, it retains the majority of quality measurements.

3.2 | Error analysis

For modern commercial lidars, the instrumental error is negligible (Sathe and Mann, 2013). The main error contributions are from random errors and systematic errors (Lenschow *et al.*, 1994). Due to the lack of reference measurements/numerical models, we calculated the relative errors (Smalikho and Banakh, 2017) of the derived EDR:

$$\text{EDR} = \sqrt{\left\langle \left(\frac{\varepsilon}{\langle\varepsilon\rangle} - 1\right)^2 \right\rangle} \times 100\% \qquad (7)$$

We calculated the 1 hr mean relative error for a general estimate, as shown in Figure 3a: from 1600 to 1700 UTC, March 24, 2017, at an altitude of around 450 m. The relative error of the EDR reaches 20.2% of the calculated EDR for a 75° elevation angle and 9.8% for a 15°
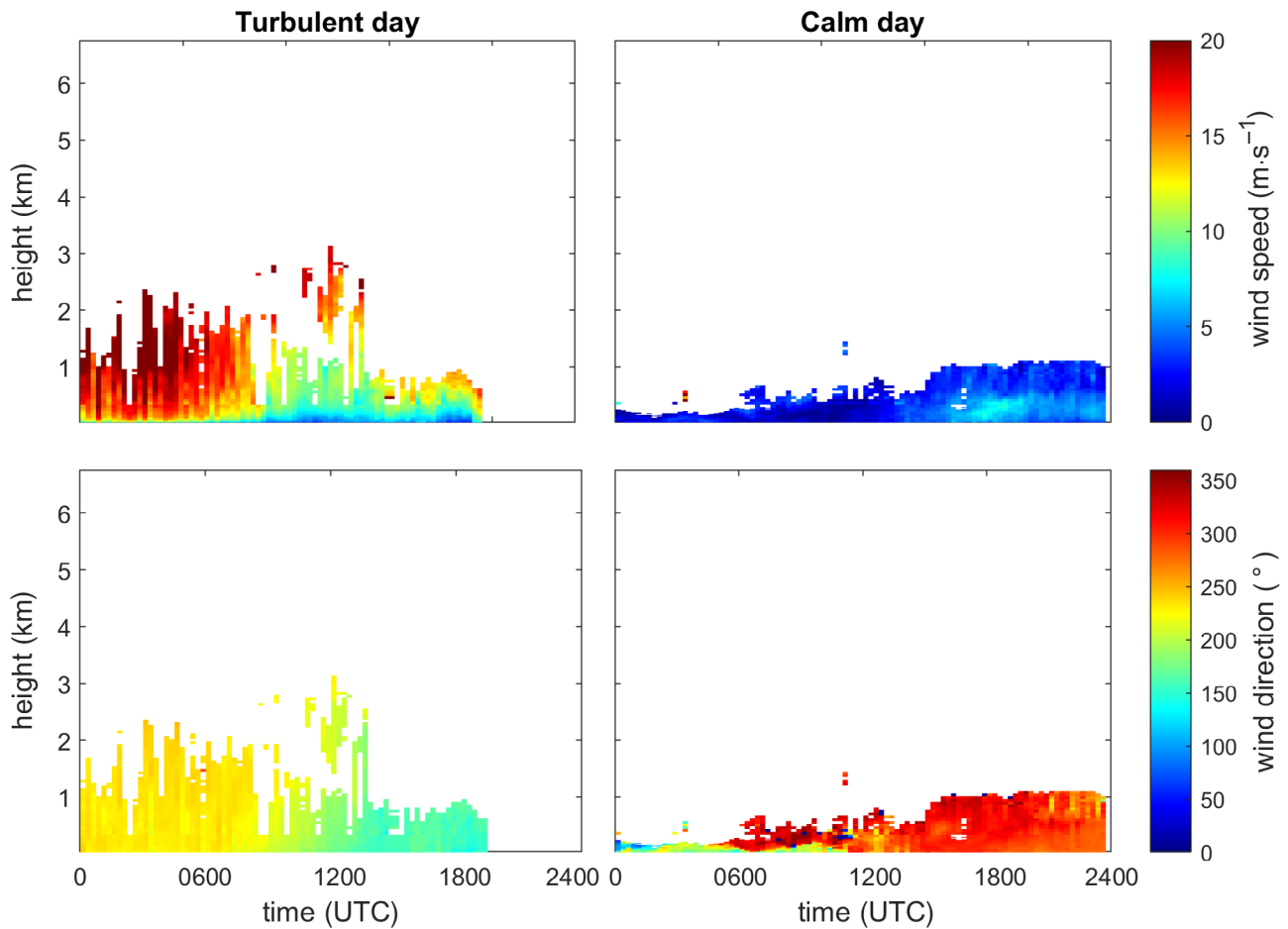
FIGURE 6 Wind speed (m·s⁻¹, top row) and wind direction (°, bottom row) measured by the lidar on March 24 (left panel) and March 31(right panel), 2017

elevation angle. These results are comparable to the results from Smalikho and Banakh (2017), which are 15%–20%. The mean relative error at the same altitude is smaller with a 15° elevation angle, which is reasonable since the 15° elevation angle has a higher R^2 value with the same CNR threshold. The poor fit to Kolmogorov's theory shown in Figure 3b has been filtered out by data screening (Section 3.1).

4 | RESULTS AND DISCUSSION

The wind fields on March 24 and March 31 are shown in Figure 6. The wind velocity on these 2 days varied significantly: on March 24, the wind direction changed from westerlies exceeding 20 m·s⁻¹ to a southerly wind of 10 m·s⁻¹; on March 31 northerly winds of 5 m·s⁻¹ dominated throughout the day.

The received lidar backscattered signal is directly related to the size and number of particles in the atmosphere. From Figure 5 and previous publications

(e.g. O'Connor et al., 2010), we know that the strongest signal comes from the well-mixed boundary layer, the height of which can vary from tens of metres to a few kilometres (Stull, 1988), and consequently the effective detection height of the lidar measurement can also vary. After applying the EDR retrieval algorithm to the lidar data, Figure 7 shows a comparison of the derived EDR on the selected dates using different scan strategies (vertical to VAD), structure functions (azimuthal to longitudinal approach), elevation angles (75° to 15°) and during different weather conditions (turbulent and calm). Note that to distinguish variations in EDR the units are shown as $\log_{10}(\varepsilon)$. As expected, the boundary layer is more extended in turbulent conditions compared to calm conditions, due to a stronger vertical mixing process. This explains why there is a clear difference in detection height between the more turbulent day (Figure 7, left panel) where the maximum detection height is about 3.5 km altitude and the calm day (Figure 7, right panel) where it is only about 1.5 km. As mentioned above, we use the VAD scans at two

FIGURE 7 Comparison of
base-10 logarithms of eddy
dissipation rate (EDR, m²·s⁻³) on a
turbulent day (March 24, 2017, left
panel) and a calm day (March
31, 2017, right panel). EDR is derived
from the vertical stare (a), (b),
velocity–azimuth display (VAD)
scans using the azimuthal approach
(azi) at 15° elevation angle (c), (d),
the azimuthal approach (azi) at 75°
elevation angle (e), (f), the
longitudinal approach (lon) at 15°
elevation angle (g), (h) and the
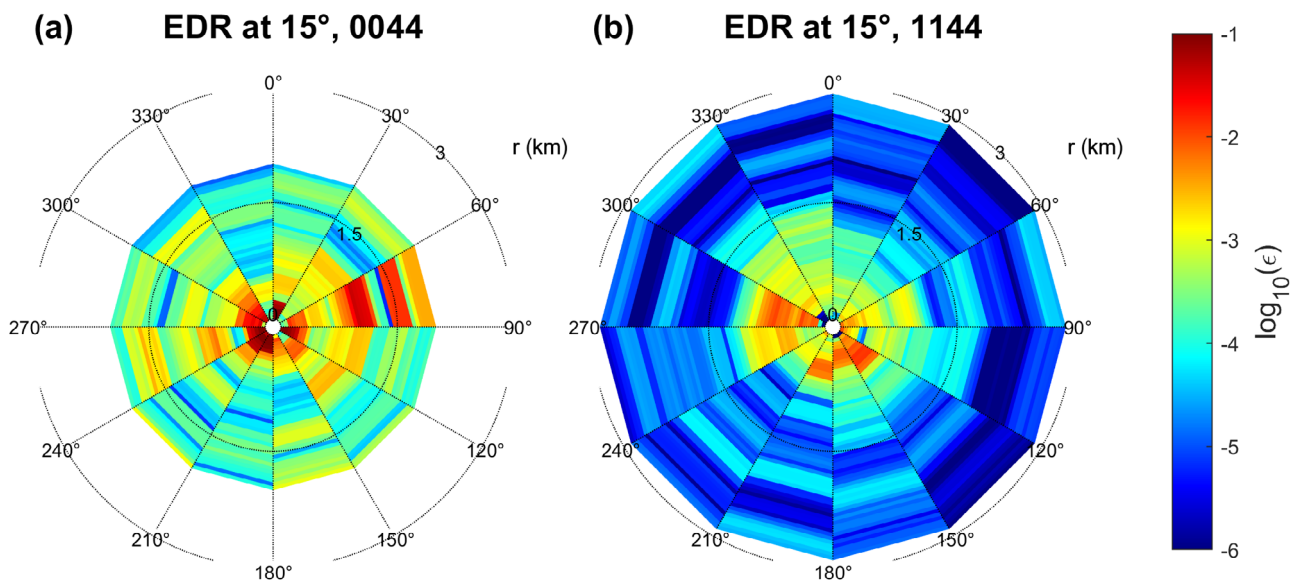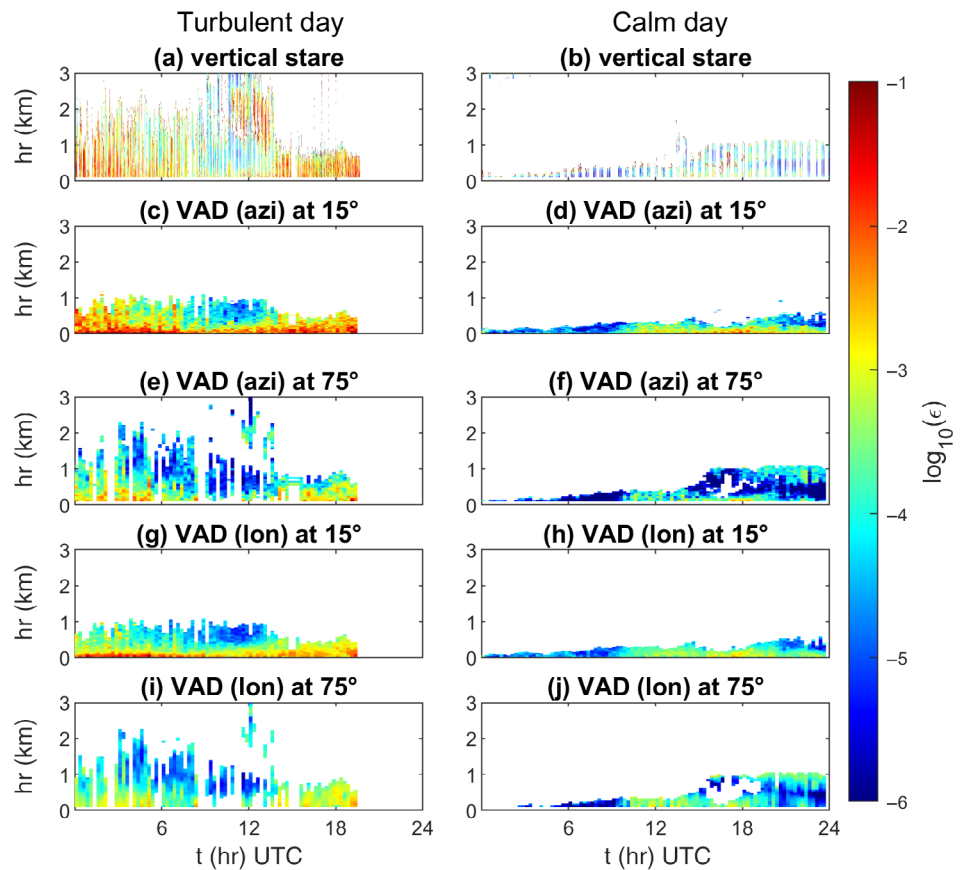longitudinal approach (lon) at 75°
elevation angle (i), (j)

FIGURE 8 Beam-circular base-10 logarithms of eddy dissipation rate (EDR, m²·s⁻³) maps for two cases at 0044 UTC (left) and 1144 UTC (right) on March 24, 2017. The data are from velocity–azimuth display (VAD) scans, at 15° elevation angle, using the longitudinal approach. The radial direction indicates the distance from the lidar. The data have been noise filtered

elevation angles, 15° and 75°. From the basic geometry, a higher elevation angle results in higher maximum and minimum detection altitude, with a constant detection range. Thus, a low elevation scan provides more

information at a lower altitude. Under optimal conditions, the lidar can retrieve a backscattered signal up to the top of the boundary layer, and additional layers of scatterers further aloft, for example the cloud around

1200 UTC on 24 March at an altitude between 2 and 3 km from Figure 7a,e,i.

As seen in Figure 7, the EDR retrievals using the structure function on VAD scans are qualitatively similar to the EDR retrievals from the vertical stares applying the method of O'Connor et al. (2010). In the early morning and afternoon of 24 March, there are high values of EDR detectable in all measurements (Figure 7, left panel), indicating turbulent conditions. During the calm day, 31 March, turbulence is detected after 1000 UTC (Figure 7, right panel), and we can also see that in the afternoon, from 1500 UTC, the top and bottom of the boundary layer was more turbulent than the middle of the boundary layer. The comparison between azimuthal (Figure 7e,f) and longitudinal (Figure 7i,j) approaches shows that they yield similar turbulence patterns, both in the turbulent and in the calm case. However, the longitudinal approach yields lower EDR values. In other words, some severe turbulent events have been underestimated. Similar results can be found with a 15° elevation angle (Figure 7c,d versus Figure 7g,h). This is more obvious in the turbulent case (24 March), when the estimated EDR from the longitudinal approach is around 14% lower than the azimuthal approach. This results from our time series analysis as we apply one more averaging calculation on the longitudinal approach than on the azimuthal approach, averaging the EDR at each range gate, to plot the altitude-to-time figure. In this approach, some turbulence will be "averaged out" or smoothened. As turbulence is a sudden change of airflow on a small temporal and spatial scale, more averaging means more smoothing. Even without a concrete validation, we can expect that the longitudinal approach may underestimate the retrieval of EDR value, at least for this time series analysis. In this regard, the azimuthal approach provides a superior EDR retrieval.

Regarding the comparison between different elevation angles, we do not expect a perfect match of the EDR because the scans at different elevation angles do not execute simultaneously. However, the results at the 15° elevation angle (Figure 7c,d) show higher EDR values than those at 75° (Figure 7e,f). One possible explanation is that, with the same range resolution, the lower elevation angle results in higher vertical resolution (12.9 m at 15° compared to 48.3 m at 75°), and we know the spatial scale of turbulence can be relatively small (dozens of metres). Thus, a low elevation angle may capture more turbulent signals compared to the same range gate with higher elevation angle. Also, the data availability at 15° scans is higher than at 75° (Figure 4). However, the heterogeneity of the atmosphere should also be considered. With a low elevation angle, range gates further along the lidar beam are also further away from the zenith position, resulting in lower representativeness and higher uncertainty. For example, at 75° elevation angle, the straight-line distance between two adjacent data points (two points at the same range gates from two adjacent beams) at 1,000 m range gate would be around 517 m, while at 15° elevation angle the distance is around 1,931 m. It is also likely that more turbulence occurs near the surface due to friction. We recommend combining both scan angles operationally: the low elevation scan for high resolution measurements at a lower altitude, and the high elevation scan for lower resolution measurements at higher altitude.

Although the azimuthal approach reveals better results for continuous time series analysis, the longitudinal approach has a potential advantage: it can retrieve EDR values along the beam, which allows us to examine where the turbulence occurs on a horizontal scale. Currently, the lidar performs two VAD scans at different elevation angles every 15 min. This enables us to monitor and locate turbulences within a certain distance, depending on the scan strategy. Figure 8 illustrates two examples of VAD scans from March 24, 2017: Figure 8a depicts the situation at 0044 UTC revealing an increased EDR to the northeast, at further range gates (1 to 2 km), while the EDR retrieved using the azimuthal approach suggests that turbulence occurred close to the lidar (Figure 7g). The second case is the situation at 1144 UTC: the atmosphere is calm at higher altitudes, that is, further along the beam, but increased EDR values are located at lower altitudes (Figure 7g). Accordingly, turbulences are found mainly to the south and west of the lidar (Figure 8b). This kind of horizontally spatial information of turbulence can only be delivered by a longitudinal approach. However, unlike the results from the azimuthal approach, which can be directly compared with results from the vertical stare (Figure 7), we are unable to compare and validate the horizontal EDR distribution for now. Nevertheless, the relative distribution of the presented EDR estimates demonstrates the potential of lidar observations to identify the location and duration of turbulence at a selected time.

Different calculation routes lead to different EDR results of the azimuthal and longitudinal approach: a single profile for the azimuthal approach and a set of conically shaped profiles for the longitudinal approach. By this means, the longitudinal approach has more potential for EDR horizontal distribution analyses, although no validation has been done so far. Regarding the temporal and vertical structure development of turbulence, the azimuthal approach performs better than the longitudinal approach, compared to vertical stare.

The VAD scan strategy can be easily modified to meet different requirements. The azimuthal interval of current

scanning is 30°, which could be decreased, but further research is needed to determine the effect on the EDR and the associated uncertainties. Further considerations would include setting up scans along airport runways. This has been done at some airports, such as Hong Kong airport (Hon and Chan, 2014).

The turbulence information we retrieved from lidar observations in the present study can be used for qualitative analyses, such as indicating the presence or absence of turbulence, but at this stage it is challenging to give a quantitative interpretation, such as how severe the turbulence is and how it would affect an airplane at take-off or landing. A validation dataset (in addition to lidar measurements) is needed, as well as input from lidar end-users, such as air traffic controllers and pilots. This may be the next step for the lidar application in Iceland.

5 | CONCLUSIONS

In this work, we investigate how Leosphere Windcube 200S Doppler lidars can be used to detect and quantify atmospheric turbulence in Iceland where the climate and weather conditions are characterized by strong winds and intense turbulence. However, the clean air (with low aerosol concentration) in Iceland leads to reduced backscatter signals from lidar systems and may require a different carrier-to-noise ratio (CNR) threshold than previous studies in other locations to screen the lidar data. Nevertheless, the present results demonstrate that our algorithm can successfully map eddy dissipation rate (EDR) over scales of several kilometres and accordingly help to monitor and identify turbulence.

Our results demonstrate that it is possible to apply velocity–azimuth display (VAD) scans and a structure function to derive near-real-time estimates of EDR. The results are comparable to EDR retrievals using vertical stares. The algorithm was able to successfully retrieve EDR for two case studies representing different typical weather conditions in Iceland, revealing the robustness of our method.

The low backscatter signal during conditions with low aerosol concentrations can lead to misinterpretations. Under these conditions (which frequently occur in Iceland), we recommend using a lower CNR threshold (−32 dB) compared to other studies and combining it with the confidence index value from the Windcube lidar.

The two approaches to calculate the structure function from the VAD scan reveal different performances: the azimuthal approach performs better in time series analysis and indicates when and at what altitude the turbulence occurs, since the longitudinal approach naturally has lower EDR values. On the other hand, the longitudinal approach shows the potential to determine the location of the turbulence relative to the lidar on a horizontal scale at a selected time, which makes it a valuable source of information near airport runways.

The EDR values vary with different VAD elevation angle. A low angle measurement has the advantage of higher data availability and quality near the surface, while a high angle measurement provides an overview at a higher altitude; thus a combination of both angles is recommended.

In general, the retrieval of EDR from lidar data to estimate the turbulence intensity is quite promising and it may be applied to improve the weather information available to the air traffic controllers in Iceland. Currently, there is ongoing work to make this algorithm operational for the lidar at Keflavik International Airport. This work has significant potential for improved aviation safety in Iceland, considering the extreme and highly variable wind conditions.

ORCID

Shu Yang https://orcid.org/0000-0001-5763-431X
Guðrún Nína Petersen https://orcid.org/0000-0003-0214-7324
David C. Finger https://orcid.org/0000-0003-0678-8946

REFERENCES

Boquet, M., Royer, P., Cariou, J.-P., Machta, M. and Valla, M. (2016) Simulation of Doppler lidar measurement range and data availability. *Journal of Atmospheric and Oceanic Technology*, 33, 977–987.

Chan, P.W. (2009) Atmospheric turbulence in complex terrain: verifying numerical model results with observations by remote-sensing instruments. *Meteorology and Atmospheric Physics*, 103, 145–157.

Chan, P.W. (2010) LIDAR-based turbulence intensity calculation using glide-path scans of the Doppler light detection and ranging (LIDAR) systems at the Hong Kong International Airport and comparison with flight data and a turbulence alerting system. *Meteorologische Zeitschrift*, 19, 549–563.

Cohn, S.A. (1994) Radar measurements of turbulent eddy dissipation rate in the troposphere: a comparison of techniques. *Journal of Atmospheric and Oceanic Technology*, 12, 85–95.

Dabas, A. (1999) Semiempirical model for the reliability of a matched filter frequency estimator for Doppler lidar. *Journal of Atmospheric and Oceanic Technology*, 16, 19–28.

Frehlich, R. (1996) Simulation of coherent Doppler lidar performance in the weak-signal regime. *Journal of Atmospheric and Oceanic Technology*, 13, 646–658.

Frehlich, R. (2001) Errors for space-based Doppler lidar wind measurements: definition, performance, and verification. *Journal of Atmospheric and Oceanic Technology*, 18, 1749–1772.

Frehlich, R. and Cornman, L. (2002) Estimating spatial velocity statistics with coherent Doppler lidar. *Journal of Atmospheric and Oceanic Technology*, 19, 355–366.

Frehlich, R., Meillier, Y., Jensen, M.L., Balsley, B. and Sharman, R. (2006) Measurements of boundary layer profiles in an urban environment. *Journal of Applied Meteorology and Climatology*, 45, 821–837.

Gryning, S.-E., Floors, R., Peña, A., Batchvarova, E. and Brümmer, B. (2016) Weibull wind-speed distribution parameters derived from a combination of wind-lidar and tall-mast measurements over land, coastal and marine sites. *Boundary-Layer Meteorology*, 159, 329–348.

Gryning, S.-E., Mikkelsen, T., Baehr, C., Dabas, A., Gómez, P., O'Connor, E., Rottner, L., Sjöholm, M., Suomi, I. and Vasiljević, N. (2017) Measurement methodologies for wind energy based on ground-level remote sensing. In: *Renewable Energy Forecasting*, pp. 29–56. Sawston, Cambridge: Elsevier.

Hocking, W.K. (1985) Measurement of turbulent energy dissipation rates in the middle atmosphere by radar techniques: a review. *Radio Science*, 20, 1403–1422.

Hon, K.K. and Chan, P.W. (2014) Application of LIDAR-derived eddy dissipation rate profiles in low-level wind shear and turbulence alerts at Hong Kong International Airport. *Meteorological Applications*, 21, 74–85.

ICAO (2018) ICAO Annual Safety Report 2018. Montreal, Canada. Available at: https://www.icao.int/safety/Documents/ICAO_SR_2018_30082018.pdf.

Kolmogorov, A.N. (1962) A refinement of previous hypotheses concerning the local structure of turbulence in a viscous incompressible fluid at high Reynolds number. *Journal of Fluid Mechanics*, 13, 82–85.

Kolmogorov, A.N. (1991) The local structure of turbulence in incompressible viscous fluid for very large Reynolds numbers. *Proceedings of the Royal Society of London*, 434, 9–13.

Lenschow, D.H., Mann, J. and Kristensen, L. (1994) How long is long enough when measuring fluxes and other turbulence statistics? *Journal of Atmospheric and Oceanic Technology*, 11, 661–673.

Leosphere, I. (2013) *WINDCUBE 100s-200s User Manual*. Orsay, France: Leosphere.

Leung, M.Y.T., Zhou, W., Shun, C.-M. and Chan, P.-W. (2018) Large-scale circulation control of the occurrence of low-level turbulence at Hong Kong International Airport. *Advances in Atmospheric Sciences*, 35, 435–444.

Manninen, A.J., Marke, T., Tuononen, M. and O'Connor, E.J. (2018) Atmospheric boundary layer classification with Doppler lidar. *Journal of Geophysical Research Atmospheres*, 123, 8172–8189.

Manninen, A.J., O'Connor, E.J., Vakkari, V. and Petäjä, T. (2016) A generalised background correction algorithm for a halo Doppler lidar and its application to data from Finland. *Atmospheric Measurement Techniques*, 9, 817–827.

Misaka, T., Ogasawara, T., Obayashi, S., Yamada, I. and Okuno, Y. (2008) Assimilation experiment of lidar measurements for wake turbulence. *Journal of Fluid Science and Technology*, 3, 512–518.

Muñoz-Esparza, D., Sharman, R.D. and Lundquist, J.K. (2018) Turbulence dissipation rate in the atmospheric boundary layer: observations and WRF mesoscale modeling during the XPIA field campaign. *Monthly Weather Review*, 146, 351–371.

Nijhuis, A.C.P.O., Unal, C.M.H., Krasnov, O.A., Russchenberg, H.W.J. and Yarovoy, A.G. (2019) Velocity-based EDR retrieval techniques applied to Doppler radar measurements from rain: two case studies. *Journal of Atmospheric and Oceanic Technology*, 36, 1693–1711.

Norris, G. (2019) Iceland's Keflavik airport reopens for restricted flight tests. Available at: https://atwonline.com/airports-routes/iceland-s-keflavik-airport-reopens-restricted-flight-tests [Accessed 1 July 2019].

O'Connor, E.J., Illingworth, A.J., Brooks, I.M., Westbrook, C.D., Hogan, R.J., Davies, F. and Brooks, B.J. (2010) A method for estimating the turbulent kinetic energy dissipation rate from a vertically pointing Doppler lidar, and independent evaluation from balloon-borne *in situ* measurements. *Journal of Atmospheric and Oceanic Technology*, 27, 1652–1664.

O'Connor, E. Research Scientist. (Personal Communication, April 2017).

Ólafsson, H. and Ágústsson, H. (2007) The Freysnes downslope windstorm. *Meteorologische Zeitschrift*, 16, 123–130.

Ólafsson, H., Furger, M. and Brümmer, B. (2007) The weather and climate of Iceland. *Meteorologische Zeitschrift*, 16, 5–8.

Pauscher, L., Vasiljevic, N., Callies, D., Lea, G., Mann, J., Klaas, T., Hieronimus, J., Gottschall, J., Schwesig, A., Kühn, M. and Courtney, M. (2016) An inter-comparison study of multi- and DBS lidar measurements in complex terrain. *Remote Sensing*, 8, 782.

Päschke, E., Leinweber, R. and Lehmann, V. (2015) An assessment of the performance of a 1.5 μm Doppler lidar for operational vertical wind profiling based on a 1-year trial. *Atmospheric Measurement Techniques*, 8, 2251–2266.

Ramanathan, V., Crutzen, P.J., Kiehl, J.T. and Rosenfeld, D. (2001) Aerosols, climate, and the hydrological cycle. *Science*, 294, 2119–2124.

Sathe, A. and Mann, J. (2013) A review of turbulence measurements using ground-based wind lidars. *Atmospheric Measurement Techniques*, 6, 3147–3167.

Sharman, R. (2016) Nature of aviation turbulence. In: Sharman, R. and Lane, T. (Eds.) *Aviation Turbulence*. Cham, Switzerland: Springer International Publishing, pp. 3–30.

Sinclair, P.C. and Kuhn, P.M. (1991) Aircraft low altitude wind shear detection and warning system. *Journal of Applied Meteorology*, 30, 3–16.

Smalikho, I.N. and Banakh, V.A. (2017) Measurements of wind turbulence parameters by a conically scanning coherent Doppler lidar in the atmospheric boundary layer. *Atmospheric Measurement Techniques*, 10, 4191–4208.

Smalikho, I., Köpp, F. and Rahm, S. (2005) Measurement of atmospheric turbulence by 2-μm Doppler lidar. *Journal of Atmospheric and Oceanic Technology*, 22, 15.

Stephan, A., Wildmann, N. and Smalikho, I.N. (2018) Spatiotemporal visualization of wind turbulence from measurements by a Windcube 200s lidar in the atmospheric boundary layer | Request PDF. In: *24th International Symposium on Atmospheric and Ocean Optics: Atmospheric Physics. Tomsk, Russian Federation: International Society for Optics and Photonics*, 1083357. Bellingham, Washington: SPIE.

Stull, R.B. (1988) *An Introduction to Boundary Layer Meteorology*. Doetinchem, Netherlands: Springer Science & Business Media.

Thobois, L.P., Krishnamurthy, R., Loaec, S., Cariou, J.P., Dolfi-Bouteyre, A., and Valla, M. (2015) Wind and EDR measurements with scanning Doppler LIDARs for preparing future weather dependent separation concepts (Invited). In: *7th AIAA*

Atmospheric and Space Environments Conference. Dallas, TX: American Institute of Aeronautics and Astronautics.

Tuononen, M., O'Connor, E.J., Sinclair, V.A. and Vakkari, V. (2017) Low-level jets over Utö, Finland, based on Doppler lidar observations. *Journal of Applied Meteorology and Climatology*, 56, 2577–2594.

Wächter, M. and Rettenmeier, A.K. (2009) Characterization of short time fluctuations in atmospheric wind speeds by LIDAR measurements. *Meteorologische Zeitschrift*, 18, 277–280.